Molecular Biology of the Cell
Vol. 21, 2674–2684, August 1, 2010

A Three-Dimensional Computer Simulation Model Reveals the Mechanisms for Self-Organization of Plant Cortical Microtubules into Oblique Arrays

Ezgi Can Eren,* Ram Dixit,† and Natarajan Gautam*

*Department of Industrial and Systems Engineering, Texas A&M University, College Station, TX 77843; and †Biology Department, Washington University, St. Louis, MO 63130

Submitted February 18, 2010; Accepted May 24, 2010
Monitoring Editor: Fred Chang

The noncentrosomal cortical microtubules (CMTs) of plant cells self-organize into a parallel three-dimensional (3D) array that is oriented transverse to the cell elongation axis in wild-type plants and is oblique in some of the mutants that show twisted growth. To study the mechanisms of CMT array organization, we developed a 3D computer simulation model based on experimentally observed properties of CMTs. Our computer model accurately mimics transverse array organization and other fundamental properties of CMTs observed in rapidly elongating wild-type cells as well as the defective CMT phenotypes observed in the *Arabidopsis mor1-1* and *fra2* mutants. We found that CMT interactions, boundary conditions, and the bundling cutoff angle impact the rate and extent of CMT organization, whereas branch-form CMT nucleation did not significantly impact the rate of CMT organization but was necessary to generate polarity during CMT organization. We also found that the dynamic instability parameters from twisted growth mutants were not sufficient to generate oblique CMT arrays. Instead, we found that parameters regulating branch-form CMT nucleation and boundary conditions at the end walls are important for forming oblique CMT arrays. Together, our computer model provides new mechanistic insights into how plant CMTs self-organize into specific 3D arrangements.

INTRODUCTION

Microtubules are dynamic polymers of tubulin subunits that assemble in a polar manner. One end of the microtubule is highly dynamic and is called the plus end, whereas the other end is either stably capped or less dynamic and is called the minus end. The function of the microtubule cytoskeleton depends on its spatial organization. In diffusely expanding plant cells, the interphase cortical microtubules (CMTs) typically form parallel arrays along the inner surface of the plasma membrane (Wasteneys and Ambrose, 2009). The overall orientation of the CMT array defines the axis of cell elongation by regulating the mechanical properties of the cell wall (Szymanski and Cosgrove, 2009). In a rapidly elongating wild-type cell, the CMT array is predominantly arranged orthogonal to the cell elongation axis, whereas in mutants that show twisted growth, the CMT array is often skewed in a handed manner (Ishida *et al.*, 2007b, but also see Sugimoto *et al.*, 2003). How the noncentrosomal plant CMTs become organized into specific 3D patterns in the absence of a central microtubule organizing center remains poorly understood.

CMTs are initiated from γ-tubulin containing nucleation complexes that are distributed throughout the plant cell cortex. Some of these nucleation complexes are associated with the sides of preexisting CMTs, and new CMTs can be seen to either branch off the "mother" CMT at acute angles (Wasteneys and Williamson, 1989a,b; Murata *et al.*, 2005; Chan *et al.*, 2009) or grow along the length of the mother CMT (Ambrose and Wasteneys, 2008; Kawamura and Wasteneys, 2008; Chan *et al.*, 2009). The CMTs are typically tightly attached to the plasma membrane (Hardham and Gunning, 1978; Barton *et al.*, 2008), which inhibits their diffusional movement and confines their polymerization dynamics to a planar surface. The minus ends of CMTs are not stably anchored to their nucleation sites and CMTs are observed to show sustained treadmilling behavior due to net growth from the plus end and net shortening from the minus end (Shaw *et al.*, 2003). This property leads to widespread displacement of CMTs during their lifetime, which results in frequent encounters between CMTs in the plane of the plasma membrane. We have previously shown that the outcome of an encounter between two CMTs depends on the contact angle. Shallow-angle encounters (<40°) typically lead to bundling of CMTs (Dixit and Cyr, 2004b). During this process, the encountering CMT changes its initial growth trajectory to coalign with the impeding CMT. In contrast, steep-angle encounters (>40°) either lead to collision-induced depolymerization of the encountering CMT (catastrophic collision) or to the encountering CMT crossing over the impeding CMT (Dixit and Cyr, 2004b). Cross-overs may subsequently trigger depolymerization of the encountering CMT due to severing at the cross-over junctions (Wightman and Turner, 2007).

In a cell, the occurrence and outcomes of CMT interactions are regulated by various microtubule-associated proteins (MAPs). Two important MAPs that regulate the organization of CMTs are encoded by the *MOR1* and *FRA2* genes. MOR1 belongs to the MAP215 family of microtubule-stabilizing factors that enhance both the growth and shortening

This article was published online ahead of print in *MBoC in Press* (http://www.molbiolcell.org/cgi/doi/10.1091/mbc.E10–02–0136) on June 2, 2010.

Address correspondence to: Ram Dixit (ramdixit@wustl.edu).

Abbreviations used: CMT, cortical microtubule; MAP, microtubule-associated protein.

rates of microtubule plus ends (Kerssemakers *et al.*, 2006; Brouhard *et al.*, 2008). The *Arabidopsis mor1-1* mutant encodes a temperature-sensitive allele that at restrictive temperatures (29–31°C) results in short, disorganized CMTs that recover their length and organization upon return to permissive temperature (21°C; Whittington *et al.*, 2001; Kawamura and Wasteneys, 2008). FRA2 is a katanin-like microtubule-severing protein that is proposed to be responsible for the release of CMTs from their nucleation sites (Wasteneys, 2002). The *Arabidopsis fra2* mutant allele encodes a truncated protein lacking 78 amino acids at the ATPase domain, which is predicted to result in complete loss of severing activity (Burk *et al.*, 2001). In this mutant, CMT organization is delayed compared with wild-type plants (Burk *et al.*, 2001; Burk and Ye, 2002).

The various interactions between CMTs are proposed to collectively result in the self-organization of an initially disorganized CMT population into a well-ordered transverse array in rapidly elongating cells (Dixit and Cyr, 2004a; Ehrhardt and Shaw, 2006; Wasteneys and Ambrose, 2009). During this process, the overall array polarity increases with CMT organization (Dixit *et al.*, 2006; Chan *et al.*, 2007). Recently, microtubule-dependent CMT nucleation was observed to show directional bias such that new CMTs predominantly face the plus end of the mother microtubule (Chan *et al.*, 2009). This process has been proposed to lead to the formation of polarized domains of CMTs during their self-organization (Chan *et al.*, 2009), but this remains to be tested experimentally.

The CMT array is a complex system in which nonintuitive dynamics are likely to be at work. To study the mechanisms at play, we previously developed a 2D computer model of CMT organization that showed that interactions between CMTs are essential for generating a parallel arrangement of CMTs (Dixit and Cyr, 2004b). Recently, other 2D computer models of CMT organization have corroborated these findings and underscored the importance of interactions between CMTs for their self-organization into an ordered array (Baulin *et al.*, 2007; Allard *et al.*, 2010). The computer model of Baulin *et al.* (2007) used a constrained CMT growth mechanism in which CMT plus ends were treated as smoothly growing structures that pause when they encounter another CMT. CMT interactions such as bundling, catastrophic collisions, and cross-over were ignored in this minimal model. Recently, Allard *et al.* (2010) used a more realistic depiction of CMT dynamics and interactions and revealed that catastrophe-inducing boundaries can bias the overall CMT organization into a single dominant orientation. However, the existing 2D computer models cannot account for 3D aspects of CMT arrays which are essential to understand how CMTs become organized in 3D plant cells.

Here, we present a 3D discrete-event simulation model that explicitly takes into account the stochastic nature of CMT dynamics and interactions by using the experimentally observed distributions of growth and shortening rates and transition probabilities for both the CMT plus and minus ends. This model also accounts for CMT interactions based on the experimentally derived contact angle distributions and frequencies of bundling, catastrophic collisions and cross-overs. Using this model, we identify the mechanisms that are critical for generating transverse CMT arrays in wild-type plants and for generating oblique arrays in mutants with twisted growth.

MATERIALS AND METHODS

Input Parameters and Boundary Conditions

We assume that the dynamic instability of all CMTs is identical in the absence of any interactions either with each other or with the boundaries. We model dynamicity at both CMT ends to capture the treadmilling mechanism. The plus end stochastically switches between growth, shortening, and pause states spending an exponentially distributed time in a given state and then transitioning to the next state according to a certain probability. In contrast, the minus end alternates between shortening and pause states spending an exponentially distributed time in each. The parameters of the exponential distribution and the transition probabilities can be easily computed based on the experimentally derived transition rates and the ratios of time spent on average in each state for a single CMT (Table S1). Each time an end of a CMT gets into a growth or shortening state, the velocities are sampled from the appropriate normal distributions derived from experimental observations (Shaw *et al.*, 2003; Kawamura and Wasteneys, 2008).

The interactions between CMTs are modeled to replicate their behavior observed in living cells. If a CMT contacts another CMT (call it a barrier) at $<40°$, it grows along the barrier CMT in the model. In this case, reorientation of the growing microtubule tip is modeled by inserting a new microtubule segment along the barrier CMT. If the contact angle is $>40°$, then 30% of the time the colliding CMT stops growing and starts to shorten (we call this a catastrophic collision), and 70% of the time it simply crosses over the barrier CMT without changing its trajectory (Wightman and Turner, 2007). If a CMT shrinks to a length of zero, it is eliminated from the system. We do not consider severing of CMTs at cross-over junctions and the possibility of stabilization of CMTs upon bundling in our model.

In most simulations, the top and bottom surfaces of the cylinders ("end walls") act as catastrophe-inducing boundaries. That is, if a CMT encounters one of those surfaces, it switches from growth to shortening (i.e., suffers a catastrophe event). We also simulate scenarios where the end walls act as reflective boundaries that do not trigger CMT shortening. In this case, when a CMT encounters an end wall its growing tip appears from the diametrically opposite point of the same end wall and maintains its normal assembly dynamics. We model this behavior by adding a microtubule segment on the other side of the end wall in the antiparallel direction which continues the growth phase of the original microtubule.

Simulations of the *mor1-1* mutant and wild-type controls use input parameters obtained at 21 and 31°C, respectively, to control for the effect of temperature on CMT assembly dynamics (Kawamura and Wasteneys, 2008).

Simulator Configuration

We developed a discrete-event simulator that is implemented in MATLAB (The Mathworks Inc., MA). A cylinder 50 μm long and 30 μm in circumference is used as a first approximation of a diffusely expanding plant cell. At the initial step, 100 CMTs of 0.1-μm length are created at locations and angles sampled from a uniform distribution. To be consistent, all CMTs are set to be in the pause state at the initial step. After the initial step, we include CMT dynamics and interactions as discussed above. Because CMTs are tightly attached to the plasma membrane along their length, we do not consider lateral and axial diffusional movement of individual CMTs in the model. New CMTs are generated according to a Poisson process with an average rate of 100 min^{-1} at locations and angles sampled from a uniform distribution. In the case of microtubule-dependent CMT nucleation, we assumed an average nucleation rate of 50 min^{-1} for both regular and microtubule-dependent CMT nucleation so that the total average rate of CMT nucleation is the same as the baseline case. In our model of an elongating plant cell, the tubulin subunit pool is assumed to not be limiting based on experimental evidence that cellular tubulin levels rise with increasing cellular growth rates (Traas *et al.*, 1984; Bustos *et al.*, 1989).

In our simulations, we keep track of *events* such as when any CMT end changes state or interacts with another CMT or a boundary. We maintain a list of events chronologically and update our snapshot of the cell from event to event. CMT growth and shortening was simulated as a tangent and then projected onto the curved 3D space of the computer-generated cylinder.

Metric for Quantifying Organization

To quantify CMT organization in a simulation and to be able to compare it to the output of another simulation, we developed a statistical metric based on Shannon's entropy formula (Shannon, 1948; Martin *et al.*, 2006). Entropy values quantify the diversity level of a system for any property of interest similar to the way they quantify the uncertainty of an information source (Gray, 1990; Balch, 2000; Lu *et al.*, 2008). We apply this entropy metric on the angle distributions of CMTs by classifying them according to their orientation and calculating the value $p_j(t)$ for each angle j which is the ratio of total length of CMTs with angle j to the total length of all CMTs. The entropy of the system at any time t, E(t) is given by the following equation:

$$E(t) = \sum_{j=1}^{180} p_j(t) \ln(p_j(t))$$

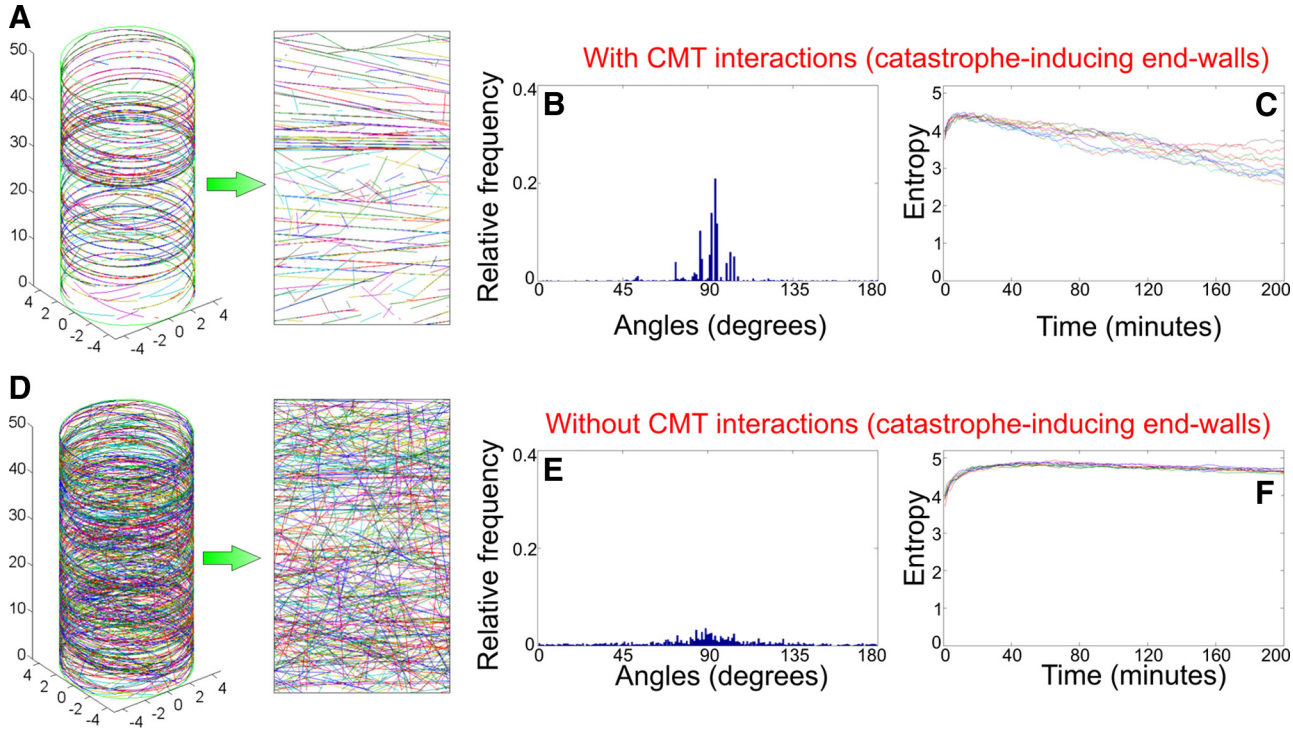

Figure 1. Comparing the effect of CMT interactions versus no CMT interactions on array organization in the presence of catastrophe-inducing boundaries. Ten independent simulations were run either considering CMT interactions or ignoring CMT interactions but using the same starting conditions. In these simulations, both the top and bottom end walls act as catastrophe-inducing boundaries. (A and D) Snapshots of two corresponding simulations taken at 200 min and their 2D representations. (B and E) Distributions of angular orientations of CMTs from the same simulations at 200 min. (C and F) Plots of entropy over time of all 10 simulations. In the presence of interactions, CMTs show a clear overall parallel organization as evidenced by a dominant peak in the angular distribution and a continuous drop in entropy. In the absence of interactions, CMTs accumulate to a higher density and show poor organization as evidenced by a more uniform angular distribution and only a slight drop in entropy. The increase in entropy at the beginning of a simulation is due to new CMTs nucleated at random locations before the existing CMTs have grown long enough to interact with each other. Note that the 2D representation of the no-interactions case highlights the visual illusion of CMT organization in the 3D snapshot.

where,

$$p_j(t) = \frac{l_j(t)}{\sum_{j=1}^{180} l_j(t)}$$

and $l_j(t)$ is the total length of CMT segments with angle j.

The entropy value approaches its maximum value of 5.19 if CMTs are perfectly uniformly distributed and approaches a theoretical value of 0 if all CMTs were to be aligned in the same direction. Note that the entropy scale is logarithmic and therefore relatively small changes in larger values of the entropy metric represent relatively large changes in CMT organization.

RESULTS

Role of CMT Interactions and Boundary Conditions during CMT Array Organization

We developed a 3D simulation model to establish the basic parameters necessary for CMT organization. We first tested what we call the *baseline* case using data shown in Table S1. In the baseline simulations, CMTs are initially scattered uniformly throughout the lateral surface of a cylindrical "cell." In these simulations, the end walls were assigned to be catastrophe-inducing (see *Materials and Methods*). The CMTs grow into a disorganized array early in the process (Movie S1). However, over time, the CMTs become longer on average, and as a result they start to interact with each other and the end walls of the cylinder, continuously transforming into better ordered arrays as seen in living cells (Figure 1A and Movie S1). An analysis of the distribution of CMT orientation angles shows that in the beginning, CMT angles are scattered akin to a uniform distribution as expected. As time passes, clustering of CMTs around a few dominant angles is seen (Figure 1B). Those dominant angles subsequently become more pronounced although they can fluctuate to some degree. Eventually, the CMTs consistently predominantly orient in a transverse direction that minimizes their frequency of colliding into the catastrophe-inducing end walls. Entropy plots show a continuous decrease in value, which indicates increased organization over time (Figure 1C).

To assess the role of interactions on CMT array organization, we modeled a scenario where CMT interactions are eliminated. In other words, all bundling and catastrophic collisions are replaced by cross-over events. We observed that CMTs fail to self-organize into ordered arrays in the absence of interactions (Movie S2). Figure 1, D and E show a snapshot and angular distribution plot for the no-interactions scenario starting with the same initial conditions as in Figure 1A. In these simulations, the slight amount of organization suggested by the weak clustering around 90° in the angle distributions and the small drop in entropy values (Figure 1F) represents the organizing effect of the catastrophe-inducing boundaries. Note that the degree of CMT array organization is hard to judge simply from the 3D snap-

shots due to the transparent surfaces of the cylinder. This is best illustrated by a side-by-side comparison of a 3D snapshot that has been "cut open" and displayed as a 2D image (Figure 1, A and D). Therefore, metrics such as angular distributions and entropy are necessary to objectively quantify the CMT array organization.

To study the effects of interactions without any interference from the boundaries, we tested another scenario where the catastrophe-inducing top and bottom end walls are replaced with reflective ones. In the absence of the catastrophe-inducing boundaries, our results show that CMTs totally fail to organize without interactions. In this case, the angular distributions stay close to uniform distribution throughout the simulation, and the entropy values never drop, but rather increase continuously to approach the maximum possible value (which is ~5.19) when CMT orientations are perfectly uniformly distributed (Figure S1, D–F). In contrast, CMT interactions alone result in self-organization similar to the baseline scenario as supported by the entropy plots (Figure S1, A–C). Thus, CMT interactions are necessary to induce self-organization regardless of the boundary conditions.

A side effect of elimination of interactions and catastrophe-inducing boundaries is that CMTs become crowded and longer because their inherent assembly dynamics are biased toward net growth (Figure 2A). The catastrophe-inducing boundaries by themselves can keep the average CMT length at a controlled level by inducing CMT catastrophe (Figure 2B). Introducing CMT interactions allows this control to take place earlier (Figure 2C) because CMTs generally start to encounter each other before they start encountering the end-wall boundaries. This observation suggests that CMT interactions and catastrophe-inducing boundaries both serve to stabilize the system. Over independent runs, the no-interactions case shows much less variability compared with the baseline (with-interactions) case for both entropy and average CMT lengths (cf. Figures 1, C and F, and 2, A and C). Increased variation between independent runs of the baseline case is especially pronounced after CMTs grow long enough to interact with each other. The variation introduced by catastrophe-inducing boundaries alone is much less pronounced.

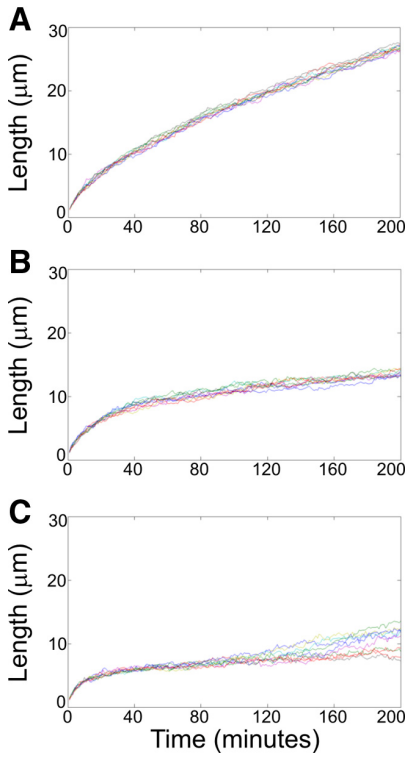

Figure 2. Analysis of the average CMT length under different conditions. Plots of the average CMT length for 10 independent simulations over 200 min are shown. (A) In the absence of both CMT interactions and catastrophe-inducing boundaries, the average CMT length is effectively unbounded and continues to increase steadily with time. (B) Simulating catastrophe-inducing boundaries alone dampens the rate of increase of the average CMT length. (C) Simulating both catastrophe-inducing boundaries and CMT interactions leads to an even greater decrease in the average CMT length till ~80 min, after which the average CMT length becomes more chaotic due to frequent interactions between CMTs.

Mutant CMT Phenotypes Are Accurately Mimicked in the Model

We tested our 3D simulation model using input data from the *Arabidopsis mor1-1* and *fra2* mutants that both show abnormal CMT organization. The *mor1-1* mutant shows normal CMT organization at 21°C, whereas at 31°C the CMTs are short and disorganized (Whittington *et al.*, 2001; Kawamura and Wasteneys, 2008). We used the experimentally derived input parameters for CMT dynamics from both wild-type and *mor1-1* mutant plants at 21 and 31°C for simulations (Table S1). We observed robust CMT organization for wild-type plants at both 21 and 31°C (Figure 3, A and B; Movie S3). In the case of the *mor1-1* mutant conditions, CMT organization occurs similar to wild-type plants at 21°C (Figure 3C). However, at 31°C, CMTs in the *mor1-1* simulations remain short and fail to organize even when the simulations are run for 1000 min (Figure 3D; Movie S4). These results agree well with the known *mor1-1* phenotype (Whittington *et al.*, 2001; Kawamura and Wasteneys, 2008) as well as with results from 2D simulations of the *mor1-1* mutant (Allard *et al.*, 2010).

We modeled the *fra2* mutant by fixing the minus ends of CMTs to their points of origin in order to simulate the loss of katanin-mediated CMT release in this mutant (Burk *et al.*, 2001; Burk and Ye, 2002; Nakamura and Hashimoto, 2009). We observed that CMT organization is slower in these simulations compared with wild-type plants, as seen from the entropy plots (cf. Figures 1C and 3E; Movie S5). This result agrees well with the known *fra2* phenotype (Burk *et al.*, 2001; Burk and Ye, 2002). Taken together, our 3D simulation model accurately mimics two mechanistically different mutant CMT phenotypes, thereby supporting the validity of our simulation model.

Relative Contribution of Bundling, Catastrophic Collisions, Catastrophe-inducing Boundaries, and Bundling Cutoff Angles to CMT Organization

The model allows us to systematically investigate the relative contribution of different parameters to CMT organization in a way that is not possible to do in living cells. Because CMT interactions are important to their organization, we tested the relative contribution of bundling and catastrophic collisions to organization. We ran two sets of simulations in which either CMT bundling or catastrophic collisions were eliminated. For each set, we ran two subsets with either catastrophe-inducing boundaries or reflective boundaries to isolate the effects of bundling and catastrophic collisions from the effects of catastrophe-inducing boundaries. For the case with no bundling, when a CMT runs into another one at an angle of <40°, it crosses over and continues its original

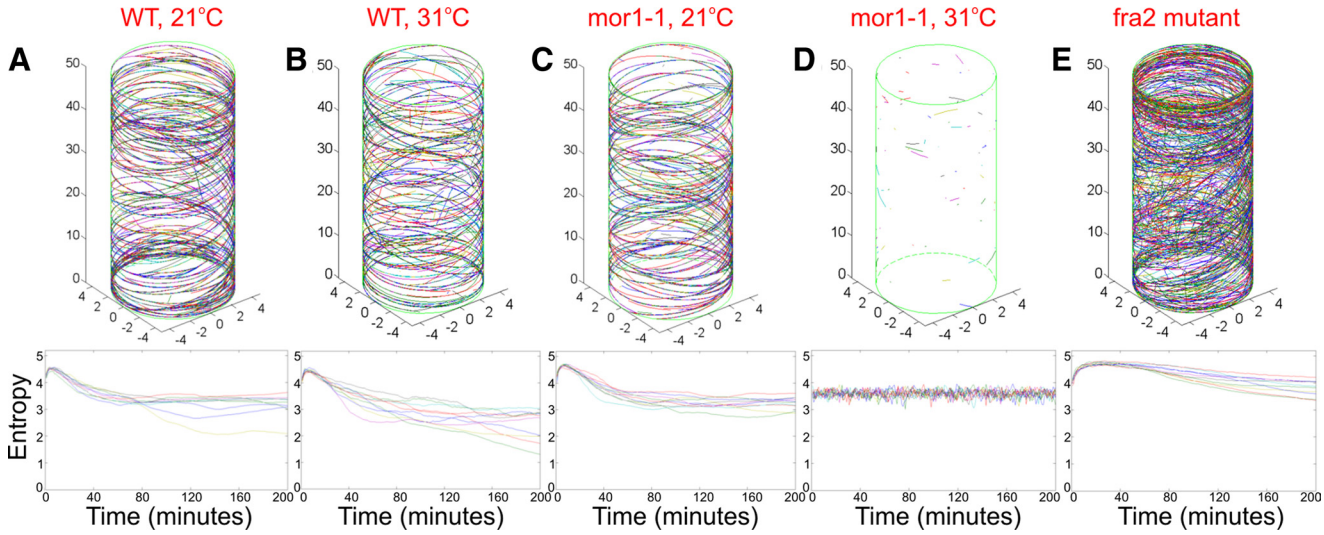

Figure 3. Simulations of *mor1-1* and *fra2 Arabidopsis* mutants. A representative snapshot at 200 min and entropy plots over time of 10 independent simulations are shown in each case. (A) Simulations of wild-type *Arabidopsis* plants at 21°C. (B) Simulations of wild-type *Arabidopsis* plants at 31°C. (C) Simulations of *mor1-1* mutant *Arabidopsis* plants at 21°C. (D) Simulations of *mor1-1* mutant *Arabidopsis* plants at 31°C. (E) Simulations of *fra2* mutant *Arabidopsis* plants. CMTs fail to become organized in the *mor1-1* mutant at 31°C and organize more slowly in the *fra2* mutant compared with wild-type controls.

trajectory. Similarly, for the case with no catastrophic collisions, collision-induced CMT shortening was replaced by cross-over at contact angles >40°.

Simulations with no bundling show much less ordering compared with baseline simulations with both bundling and catastrophic collisions regardless of boundary conditions (Figure 4, A and C). Eliminating catastrophic collisions does not have a significant effect on CMT organization in the presence of catastrophe-inducing boundaries (Figure 4B) but does slightly inhibit CMT organization when the catastrophe-inducing boundaries are replaced by reflective ones (Figure 4D). These data indicate that self-organization

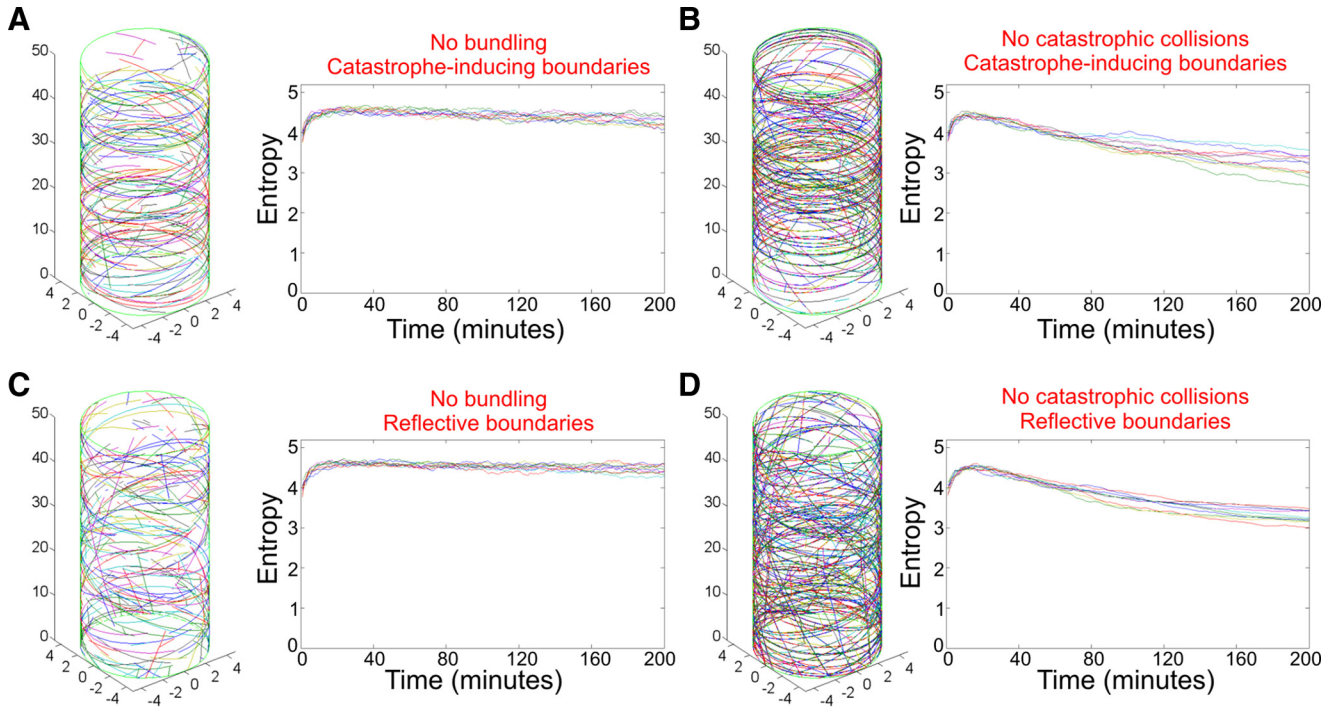

Figure 4. Relative importance of bundling and catastrophic collisions to CMT organization. Ten independent simulations were run either with catastrophe-inducing boundaries (A and B) or with reflective boundaries (C and D). In each case, a representative snapshot at 200 min and entropy plots of all 10 runs are shown. The absence of CMT bundling prevents CMT organization regardless of the boundary conditions (A and C). The absence of catastrophic collisions does not matter much if the end walls act as catastrophe-inducing boundaries (B), but it does slightly reduce organization if the end walls act as reflective boundaries (D).

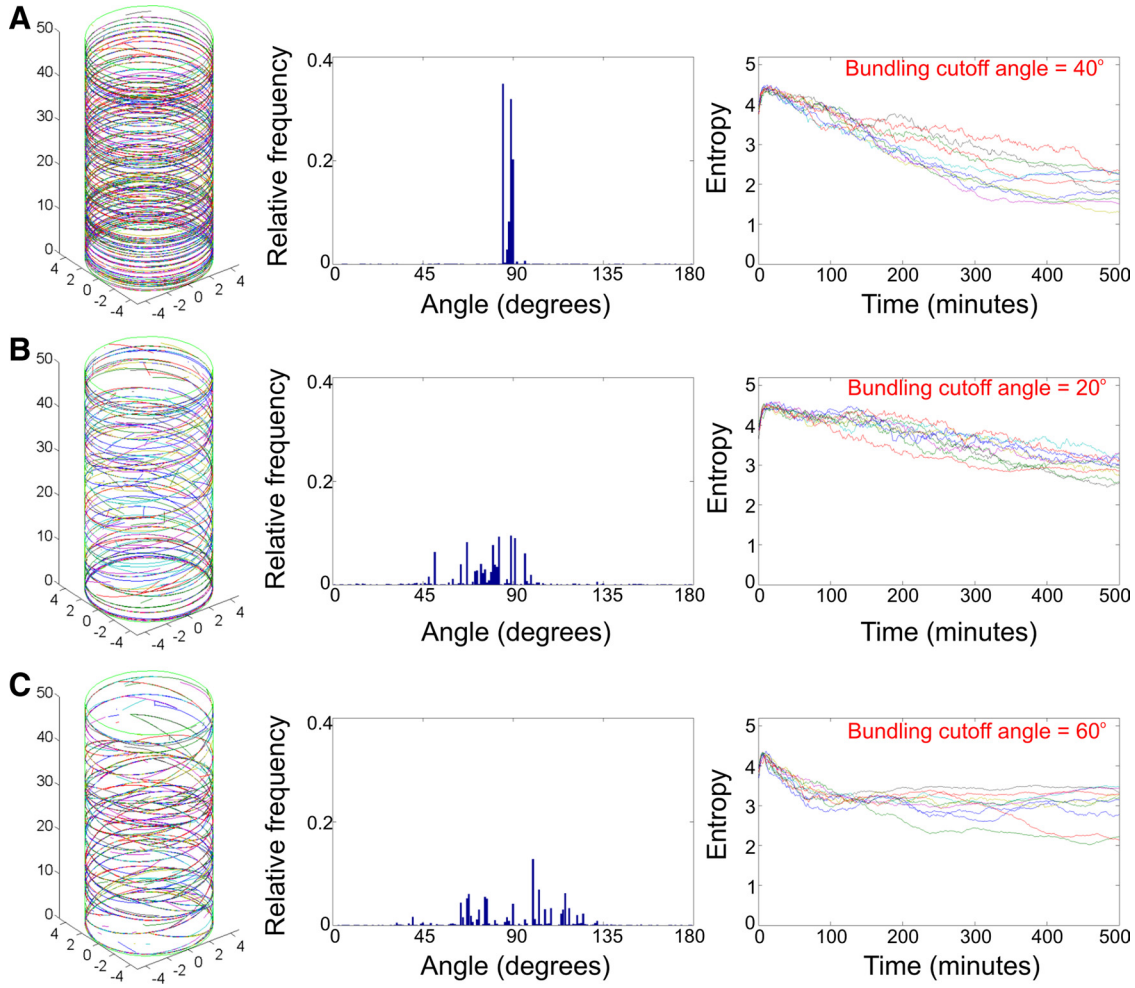

Figure 5. Effect of the cutoff angle for CMT bundling on the organization of the CMT array. The same starting conditions from 10 independent simulations were used for all experiments. In each case, a representative snapshot at 500 min, the angular distribution of CMTs at 500 min and entropy plots for all 10 runs are shown. (A) At a bundling cutoff angle of 40°, CMTs consistently organize into well-ordered transverse arrays as judged from their angular distributions and entropy plots. (B) At a bundling cutoff angle of 20°, the organization of the CMTs is inhibited compared with the controls. (C) At a bundling cutoff angle of 60°, CMTs initially show more rapid organization but later stabilize at a higher entropy level compared with the controls. Data are shown over 500 min to emphasize that the higher entropy levels due to the 60° bundling cutoff angle is not transient.

of CMTs is better and faster when all three factors are present.

In our model, small changes in the cutoff angle that leads to bundling did not affect CMT organization. For example, changing the cutoff angle to 45° did not significantly affect organization compared with the baseline case, which used 40° as the cutoff angle (data not shown). However, larger changes in cutoff angle do impact CMT organization. If the cutoff angle is 20°, the CMTs remain relatively short and organize poorly compared with control simulations (cf. Figure 5, A and B). On the other hand, if the cutoff angle is 60°, the CMTs grow longer on average and initially show faster organization but then stabilize at a higher entropy value compared with control simulations (cf. Figure 5, A and C). In these experiments, we adjusted the catastrophe frequency so that it is similar to the baseline case in order to more reliably evaluate the contribution of bundling angle.

Microtubule-based CMT Nucleation Contributes to Array Polarity

In plant cells, well-ordered transverse CMT arrays show an overall net polarity, where ~80% of the CMTs grow toward the same direction (Dixit *et al.*, 2006). Our baseline conditions are not sufficient to induce such polarity (Figure 6A). We introduced microtubule-dependent CMT nucleation in our simulations to test if it affects array polarity during CMT organization. We simulated microtubule-dependent nucleation using data from Chan *et al.* (2009). Specifically, a new CMT is nucleated along the side of an existing CMT and grows either along its mother CMT (38% of the time) or at an acute angle (62% of the time), which is called the branch angle. The branch angle is sampled from a distribution with a mean of 40° based on available experimental data (Murata *et al.*, 2005; Chan *et al.*, 2009). Branching to the left or right side of the mother CMT is equally likely and the new CMTs originate with their plus ends facing toward the plus end of the mother CMT (Chan *et al.*, 2009). We assume that the point of nucleation is uniformly distributed among the existing growing segments of CMTs. For these simulations, we set the average rate for both regular and branched nucleation at 50 min^{-1}, so that the total average nucleation rate stays the same as our baseline scenario.

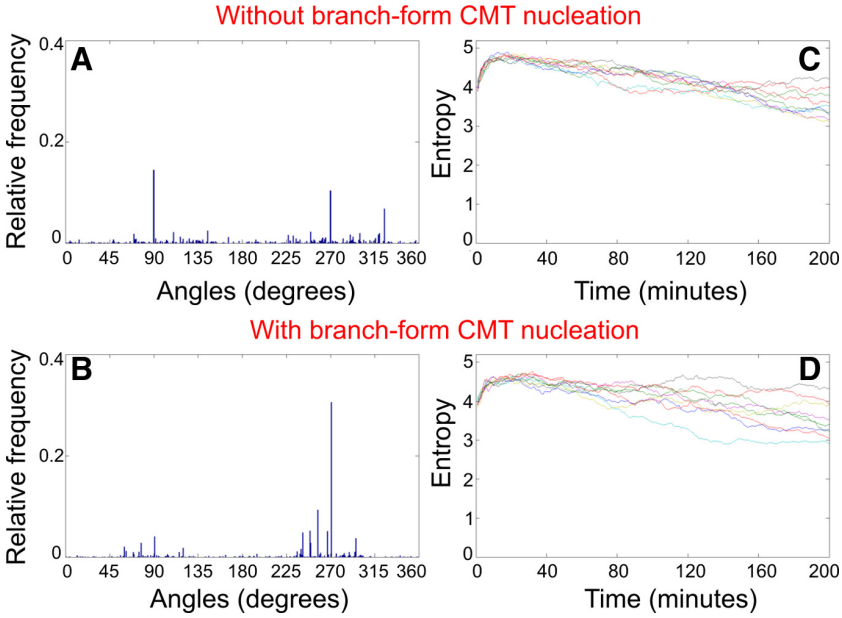

Figure 6. Emergence of net array polarity due to branch-form CMT nucleation. A representative distribution of the absolute angular orientations of CMTs and entropy plots for 10 independent simulations are shown for baseline conditions (A and C) and using branch-form CMT nucleation (B and D). Under baseline conditions, there is no appreciable array polarity quantified as the difference in percent CMTs oriented at 90° and at 270° (A). Simulating branch-form CMT nucleation results in ~70% net polarity (B). Entropy plots show that branch-form CMT nucleation introduces greater variability (D) compared with the baseline case (C). However, the average rate and level of CMT organization is similar with and without branch-form CMT nucleation.

Our results show that branched nucleation, regardless of the boundary conditions, significantly increases the frequency of observing net array polarity in ordered CMT arrays. More than half of the simulations in 10 independent runs showed ~75% bias in one direction (Figure 6B), whereas the remaining runs showed a more modest 60% bias in one direction. We note that branched nucleation did not significantly impact the rate or degree of CMT organization compared with the baseline experiments (Figure 6, C and D).

Identification of Potential Mechanisms That Skew CMT Arrays in a Handed Manner

We were particularly interested in the mechanisms that lead to oblique CMT arrays such as those described in many mutants that show twisted growth (Furutani *et al.*, 2000; Thitamadee *et al.*, 2002; Buschmann *et al.*, 2004; Nakajima *et al.*, 2004, 2006; Ishida *et al.*, 2007a; Yao *et al.*, 2008; Buschmann *et al.*, 2009; Nakamura and Hashimoto, 2009; Sunohara *et al.*, 2009). Many of the twisted growth mutants have altered CMT assembly dynamics but it is not known whether the changes in CMT dynamics contribute to the formation of an oblique CMT array (Ishida *et al.*, 2007a; Yao *et al.*, 2008; Buschmann *et al.*, 2009). To determine if defective CMT dynamics can change the overall pitch of the CMT array, we simulated the dynamic instability parameters of the $tua4^{S178\Delta}$ and $tua5^{D251N}$ mutants that, respectively, show right- and left-handed skewed CMT arrays (Ishida *et al.*, 2007a). These mutations affect genes (*TUA4* and *TUA5*) encoding the α-tubulin subunits that make up the CMT polymer (Ishida *et al.*, 2007a). Our results show that the CMT dynamics of the $tua4^{S178\Delta}$ mutant results in short CMTs that fail to become organized (Figure S2A). Similarly, the CMT dynamics of the $tua5^{D251N}$ mutant results in relatively poorly organized CMT arrays that do not exhibit skewing (Figure S2B). Thus, the defective CMT assembly dynamics of the $tua4^{S178\Delta}$ and $tua5^{D251N}$ mutants cannot explain how oblique CMT arrays are formed in these plants.

To explore possible mechanisms that are responsible for oblique CMT arrays, we simulated the following scenarios: 1) An increase or decrease in the mean branch angle on both sides of the mother CMT during microtubule-dependent CMT nucleation; 2) Introducing a bias for one side of the mother CMT during microtubule-dependent CMT nucleation (i.e., nucleation on either the left or the right of the mother CMT); 3) An increase or decrease in the mean branch angle on only one side of the mother CMT during microtubule-dependent CMT nucleation; and 4) Assigning only one of the end walls of the cylinder as a catastrophe-inducing boundary. Note that microtubule-dependent CMT nucleation is included in all of these scenarios.

In these experiments, we defined an oblique array as one that shows at least a 20° shift from the transverse orientation. This is a conservative definition based on the average skewing angle of ~10° reported in twisted growth mutants (Furutani *et al.*, 2000; Abe *et al.*, 2004; Buschmann *et al.*, 2004, 2009; Ishida *et al.*, 2007a; Yao *et al.*, 2008; Nakamura and Hashimoto, 2009). Our results show that all of the tested mechanisms increase the probability of oblique CMT array formation compared with control experiments without these modifications (Figure 7 and Table S2). Changing the boundary conditions and the mean branching angle on either one side or both sides of a mother CMT were found to be particularly potent at changing the pitch of the CMT array (Movies S6–S8). These conditions however did not skew CMT arrays with a fixed handedness.

We tested if the extent and timing of branch-form CMT assembly can confer fixed handedness during skewing of CMT arrays based on a model proposed by Wasteneys and Ambrose (2009). The scenario that worked best involved first allowing CMTs to organize into a transverse array in the absence of microtubule-dependent CMT nucleation followed by a switch to 100% branch-form CMT nucleation. Under these conditions, we obtained oblique arrays that consistently skewed in the same direction (Figure 8 and Movie S9). We note that inclusion of CMT nucleation along the mother CMT (38% of the total microtubule-dependent nucleation) in this scenario disrupted the formation of oblique CMT arrays. We also note that selective elimination of the mother CMTs following branch-form nucleation as proposed by Wasteneys and Ambrose (2009) was not neces-

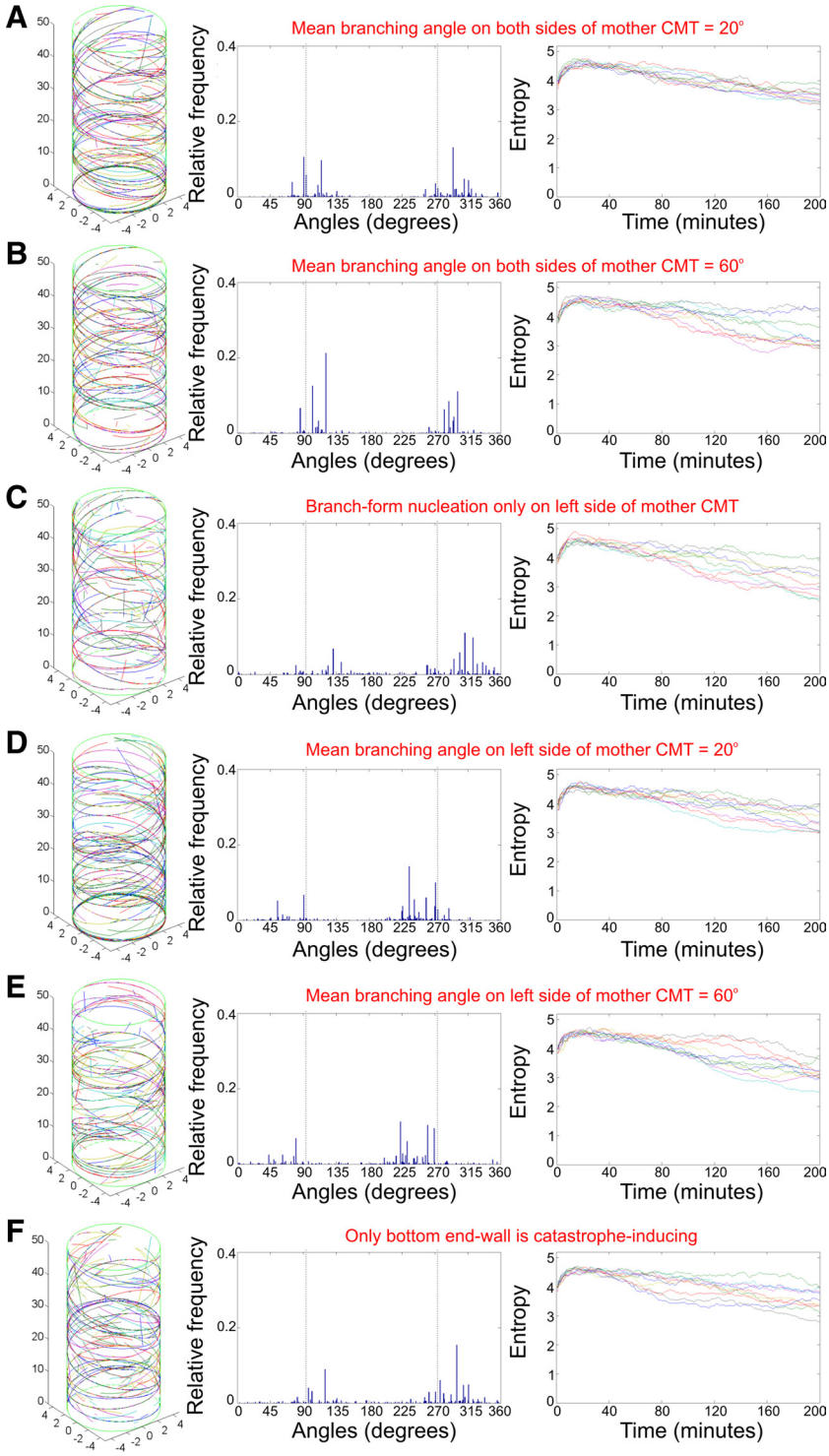

Figure 7. Formation of oblique CMT arrays. In each case, a representative snapshot at 200 min, the concomitant distribution of the absolute angular orientations of CMTs and entropy plots of 10 independent simulations are shown. A CMT array is considered to be oblique if the dominant angular orientation is shifted by at least 20° from the transverse orientation (indicated by the dotted lines). (A) Simulation in which the mean angle for branch-form CMT nucleation is 20° on both sides of a mother CMT. (B) Simulation in which the mean angle for branch-form CMT nucleation is 60° on both sides of a mother CMT. (C) Simulation in which branch-form CMT nucleation occurs only on the left side of a mother CMT. (D) Simulation in which the mean angle for branch-form CMT nucleation is 20° only on the left side of a mother CMT. (E) Simulation in which the mean angle for branch-form CMT nucleation is 60° only on the left side of a mother CMT. (F) Simulation in which only the bottom end wall behaves as a catastrophe-inducing boundary.

sary for array skewing and in fact led to rapid depletion of the whole microtubule population.

DISCUSSION

In this work, we developed a 3D computer simulation model to identify the parameters that control the self-organization of CMTs in a setting that approximates a 3D plant cell. Our model explicitly considers the stochastic nature of CMT dynamics as well as the various modes of interactions between CMTs in order to closely mimic the behavior of CMTs in living cells. Indeed, outputs from our baseline simulations (that mimic wild-type cells) closely match many basic properties of CMTs observed in real cells: 1 The average length of CMTs is ~10 μm in our simulations, which is similar to the reported average CMT length of 8.6–12.4 μm in plant cells (Barton *et al.*, 2008); 2 The CMTs typically grow in a shallow arc-like trajectory along the cylindrical cell surface as ob-

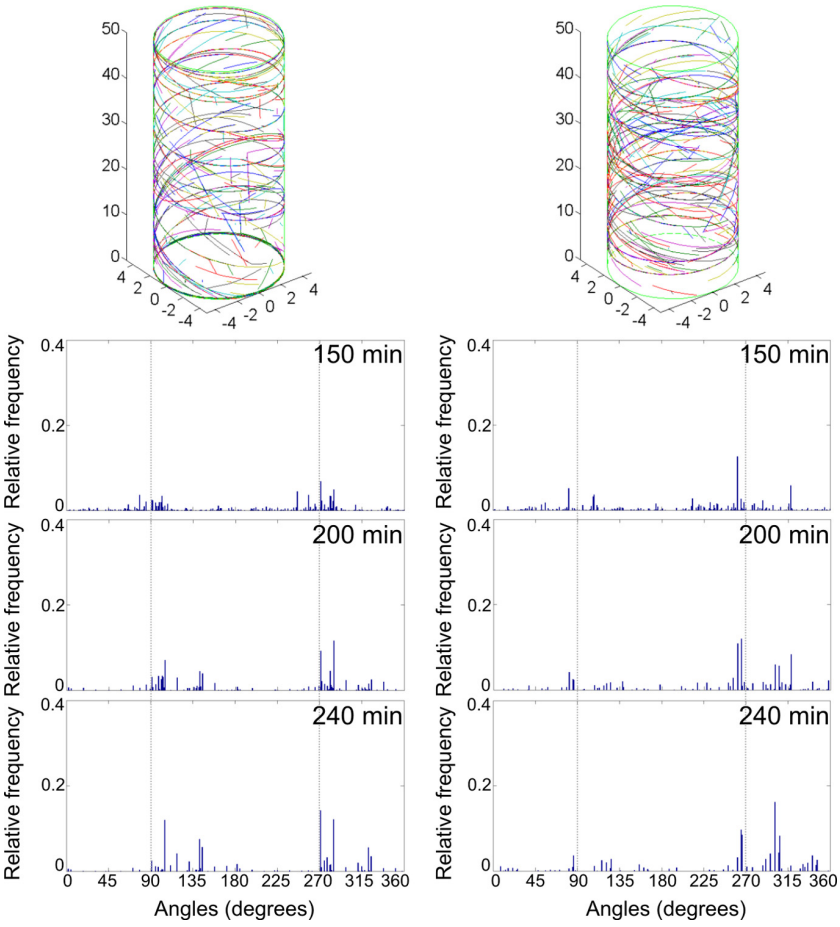

Figure 8. Generating oblique CMT arrays with fixed handedness. Two representative snapshots at 240 min and respective distributions of the absolute angular orientations of CMTs from 10 independent simulations are shown. In these simulations, new CMTs were generated at random locations without any branch-form CMT nucleation for the first 150 min. After 150 min, new CMTs were generated exclusively through branch-form nucleation at a branching angle of 40°. The dotted lines in the angular distributions indicate the transverse orientation. These simulation conditions consistently result in left-handed skewed CMT arrays.

served in real plant cells (Shaw *et al.*, 2003; Wightman and Turner, 2007); 3 Entropy decreases smoothly in our simulations, indicating that CMT organization proceeds progressively and not discontinuously similar to the observations in real cells (Yuan *et al.*, 1994; Granger and Cyr, 2001; Dixit *et al.*, 2006); 4 Stable CMT organization is observed by about 120–150 min in our simulations, which agrees with the time to organization of ~120 min in plant cells (Wasteneys and Williamson, 1989a; Dixit *et al.*, 2006); and 5 Local domains of high organization dynamically emerge in our simulations as described in real cells (Marc *et al.*, 1998; Dixit *et al.*, 2006; Chan *et al.*, 2007).

In addition, our model accurately mimicked the CMT phenotypes of the *mor1-1* and *fra2* mutants by using experimental data derived from these mutants as inputs for the simulations. Our results show that defective CMT dynamics at 31°C in the *mor1-1* mutant are sufficient for disrupting CMT organization. This observation confirms similar results obtained by Allard *et al.* (2010) using 2D computer simulations. In addition, our results from the *fra2* mutant simulations show that release from nucleation sites and minus-end dynamics are not essential for generating CMT organization but rather that they contribute to the speed of organization.

We consistently observed that interactions between CMTs are necessary for parallel CMT organization as reported previously using 2D simulations (Dixit and Cyr, 2004b; Baulin *et al.*, 2007; Allard *et al.*, 2010). Interestingly, interactions between CMTs lead to increased variability in the average CMT length and entropy between independent simulations compared with control simulations with no interactions. Minor perturbations to the frequency of CMT interactions did not significantly dampen the observed fluctuations in average CMT length and entropy during array organization. These findings illustrate two interesting features: 1 CMT organization is extremely robust to minor changes in interaction frequency although exhibiting a chaotic behavior with respect to average CMT length and entropy; and 2 If the change in CMT interaction frequency is huge, then both organization as well as the chaotic behavior are lost.

Based on our results, we conclude that bundling of CMTs is a major driving force for parallel CMT organization in agreement with Allard *et al.* (2010). In comparison, catastrophic collisions and catastrophe-inducing boundaries are minor contributors to parallel CMT organization. However, the combined action of bundling, catastrophic collisions and catastrophe-inducing boundaries was observed to lead to faster and better CMT organization compared with simulations that lacked any of these parameters. This finding suggests that multiple mechanisms are likely operating to generate CMT organization in cells.

Experimentally, the bundling cutoff angle is ~40° in wild-type plant cells (Dixit and Cyr, 2004b; Wightman and Turner, 2007; Ambrose and Wasteneys, 2008). We found that major deviations from this cutoff angle have pronounced effects on CMT organization. At a bundling cutoff angle of 20°, CMTs organized more slowly compared with control simulations because fewer CMTs became bundled. If the bundling cutoff angle was increased to 60°, entropy decreased quickly early in the simulations but stabilized around a significantly higher value compared with control

simulations contrary to our expectations. Therefore, increasing bundling beyond a certain level is detrimental to the long-term CMT organization and supports the idea that a balance between different types of CMT interactions is important for proper CMT organization (Wasteneys and Ambrose, 2009).

Well-ordered CMT arrays show a net array polarity (Dixit *et al.*, 2006; Chan *et al.*, 2007). We found that simulating microtubule-dependent CMT nucleation is necessary to develop array polarity during CMT organization. This result supports the hypothesis that a directional bias in microtubule-dependent CMT nucleation leads to the self-perpetuation of CMTs that share the same polarity during CMT organization (Chan *et al.*, 2009).

In our baseline experiments, the CMT array was consistently oriented predominantly in the transverse direction. It has been proposed that changes in CMT dynamics play a major role in skewing the CMT array away from a transverse direction (Ishida *et al.*, 2007a). However, our results show that the defective CMT assembly dynamics in mutants with twisted growth cannot account for skewing of the CMT arrays. Interestingly, the altered CMT assembly dynamics of the $tua4^{S178\Delta}$ mutant result in short, disorganized CMTs similar to the *mor1-1* mutant at restrictive temperature. Both $tua4^{S178\Delta}$ and *mor1-1* show left-handed organ twisting (Whittington *et al.*, 2001; Ishida *et al.*, 2007a), indicating that twisted growth does not require a skewed CMT array.

Our results predict that parameters that govern branch-form CMT nucleation and boundary conditions at the end walls are important for skewing of CMT arrays. Interestingly, using modified nucleation and boundary condition parameters throughout a simulation did not result in skewing of the CMT arrays a 100% of the time nor did they result in skewing with fixed handedness. On the other hand, a switch to branch-form CMT nucleation after formation of a transverse array skews CMT arrays consistently in the same direction. Together, our data support the idea that the extent of branch-form nucleation and its timing serve to regulate the overall pitch of the CMT array in plant cells (Wasteneys and Ambrose, 2009).

Several predictions of our model are supported by available experimental evidence. One prediction is that an increase in the mean branch angle of CMT nucleation will result in oblique CMT arrays. This prediction is supported by the observation that in the *Arabidopsis spiral3* mutant, skewing of the CMT array is not correlated with altered CMT assembly dynamics and nucleation rate but rather is correlated with an increase in the mean angle during branch-form CMT nucleation (Nakamura and Hashimoto, 2009). Another prediction of our model is that a mean branch angle of 20° will improve parallel CMT organization as judged by the consistently low entropy values between independent simulations. This prediction is supported by the finding that in mutant *Arabidopsis* plants with a compromised GCP4 function, an increase in parallel CMT organization is correlated to a mean branch angle of ~27° (Kong *et al.*, 2010). Taken together, our computer model offers new insights into the fundamental mechanisms that are important for the 3D organization of the plant CMT array.

ACKNOWLEDGMENTS

The authors acknowledge that this work greatly benefitted from the numerous discussions with Drs. Richard Cyr and Abhijit Deshmukh.

REFERENCES

Abe, T., Thitamadee, S., and Hashimoto, T. (2004). Microtubule defects and cell morphogenesis in the lefty1lefty2 tubulin mutant of *Arabidopsis thaliana*. Plant Cell Physiol. *45*, 211–220.

Allard, J. F., Wasteneys, G. O., and Cytrynbaum, E. N. (2010). Mechanisms of self-organization of cortical microtubules in plants revealed by computational simulations. Mol. Biol. Cell *21*, 278–286.

Ambrose, J. C., and Wasteneys, G. O. (2008). CLASP modulates microtubule-cortex interaction during self-organization of acentrosomal microtubules. Mol. Biol. Cell *19*, 4730–4737.

Balch, T. (2000). Hierarchic social entropy: an information theoretic measure of robot group diversity. Autonomous Robots *8*, 209–237.

Barton, D. A., Vantard, M., and Overall, R. L. (2008). Analysis of cortical arrays from *Tradescantia virginiana* at high resolution reveals discrete microtubule subpopulations and demonstrates that confocal images of arrays can be misleading. Plant Cell *20*, 982–994.

Baulin, V. A., Marques, C. M., and Thalmann, F. (2007). Collision induced spatial organization of microtubules. Biophys. Chem. *128*, 231–244.

Brouhard, G. J., Stear, J. H., Noetzel, T. L., Al-Bassam, J., Kinoshita, K., Harrison, S. C., Howard, J., and Hyman, A. A. (2008). XMAP215 is a processive microtubule polymerase. Cell *132*, 79–88.

Burk, D. H., Liu, B., Zhong, R., Morrison, W. H., and Ye, Z. H. (2001). A katanin-like protein regulates normal cell wall biosynthesis and cell elongation. Plant Cell *13*, 807–827.

Burk, D. H., and Ye, Z. H. (2002). Alteration of oriented deposition of cellulose microfibrils by mutation of a katanin-like microtubule-severing protein. Plant Cell *14*, 2145–2160.

Buschmann, H., Fabri, C. O., Hauptmann, M., Hutzler, P., Laux, T., Lloyd, C. W., and Schaffner, A. R. (2004). Helical growth of the *Arabidopsis* mutant tortifolia1 reveals a plant-specific microtubule-associated protein. Curr. Biol. *14*, 1515–1521.

Buschmann, H., Hauptmann, M., Niessing, D., Lloyd, C. W., and Schaffner, A. R. (2009). Helical growth of the *Arabidopsis* mutant tortifolia2 does not depend on cell division patterns but involves handed twisting of isolated cells. Plant Cell *21*, 2090–2106.

Bustos, M. M., Guiltinan, M. J., Cyr, R. J., Ahdoot, D., and Fosket, D. E. (1989). Light Regulation of beta-tubulin gene expression during internode development in soybean (*Glycine max* [L.] Merr.). Plant Physiol. *91*, 1157–1161.

Chan, J., Calder, G., Fox, S., and Lloyd, C. (2007). Cortical microtubule arrays undergo rotary movements in *Arabidopsis* hypocotyl epidermal cells. Nat. Cell Biol. *9*, 171–175.

Chan, J., Sambade, A., Calder, G., and Lloyd, C. (2009). *Arabidopsis* cortical microtubules are initiated along, as well as branching from, existing microtubules. Plant Cell *21*, 2298–2306.

Dixit, R., Chang, E., and Cyr, R. (2006). Establishment of polarity during organization of the acentrosomal plant cortical microtubule array. Mol. Biol. Cell *17*, 1298–1305.

Dixit, R., and Cyr, R. (2004a). The cortical microtubule array: from dynamics to organization. Plant Cell *16*, 2546–2552.

Dixit, R., and Cyr, R. (2004b). Encounters between dynamic cortical microtubules promote ordering of the cortical array through angle-dependent modifications of microtubule behavior. Plant Cell *16*, 3274–3284.

Ehrhardt, D. W., and Shaw, S. L. (2006). Microtubule dynamics and organization in the plant cortical array. Annu. Rev. Plant Biol. *57*, 859–875.

Furutani, I., Watanabe, Y., Prieto, R., Masukawa, M., Suzuki, K., Naoi, K., Thitamadee, S., Shikanai, T., and Hashimoto, T. (2000). The SPIRAL genes are required for directional control of cell elongation in *Arabidopsis thaliana*. Development *127*, 4443–4453.

Granger, C. L., and Cyr, R. J. (2001). Spatiotemporal relationships between growth and microtubule orientation as revealed in living root cells of *Arabidopsis thaliana* transformed with green-fluorescent-protein gene construct GFP-MBD. Protoplasma *216*, 201–214.

Gray, R. M. (1990). Entropy and Information Theory, Springer-Verlag: New York.

Hardham, A. R., and Gunning, B. E. (1978). Structure of cortical microtubule arrays in plant cells. J. Cell Biol. *77*, 14–34.

Ishida, T., Kaneko, Y., Iwano, M., and Hashimoto, T. (2007a). Helical microtubule arrays in a collection of twisting tubulin mutants of *Arabidopsis thaliana*. Proc. Natl. Acad. Sci. USA *104*, 8544–8549.

Ishida, T., Thitamadee, S., and Hashimoto, T. (2007b). Twisted growth and organization of cortical microtubules. J. Plant Res. *120*, 61–70.

Kawamura, E., and Wasteneys, G. O. (2008). MOR1, the *Arabidopsis thaliana* homologue of *Xenopus* MAP215, promotes rapid growth and shrinkage, and suppresses the pausing of microtubules in vivo. J. Cell Sci. *121*, 4114–4123.

Kerssemakers, J. W., Munteanu, E. L., Laan, L., Noetzel, T. L., Janson, M. E., and Dogterom, M. (2006). Assembly dynamics of microtubules at molecular resolution. Nature *442*, 709–712.

Kong, Z., Hotta, T., Lee, Y.R., Horio, T., and Liu, B. (2010). The γ-tubulin complex protein GCP4 is required for organizing functional microtubule arrays in *Arabidopsis thaliana*. Plant Cell *22*, 191–204.

Lu, J. L., Valois, F., Dohler, M., and Barthel, D. (2008). Quantifying organization by means of entropy. IEEE Commun. Lett. *12*, 185–187.

Marc, J., Granger, C. L., Brincat, J., Fisher, D. D., Kao, T., McCubbin, A. G., and Cyr, R. J. (1998). A GFP-MAP4 reporter gene for visualizing cortical microtubule rearrangements in living epidermal cells. Plant Cell *10*, 1927–1940.

Martin, M. T., Plastinoa, A., and Rossob, O. A. (2006). Generalized statistical complexity measures: geometrical and analytical properties. Physica A *369*, 439–462.

Murata, T., Sonobe, S., Baskin, T. I., Hyodo, S., Hasezawa, S., Nagata, T., Horio, T., and Hasebe, M. (2005). Microtubule-dependent microtubule nucleation based on recruitment of gamma-tubulin in higher plants. Nat. Cell Biol *7*, 961–968.

Nakajima, K., Furutani, I., Tachimoto, H., Matsubara, H., and Hashimoto, T. (2004). SPIRAL1 encodes a plant-specific microtubule-localized protein required for directional control of rapidly expanding *Arabidopsis* cells. Plant Cell *16*, 1178–1190.

Nakajima, K., Kawamura, T., and Hashimoto, T. (2006). Role of the SPIRAL1 gene family in anisotropic growth of *Arabidopsis thaliana*. Plant Cell Physiol. *47*, 513–522.

Nakamura, M., and Hashimoto, T. (2009). A mutation in the *Arabidopsis* gamma-tubulin-containing complex causes helical growth and abnormal microtubule branching. J. Cell Sci. *122*, 2208–2217.

Shannon, C. E. (1948). A mathematical theory of communication. Bell System Tech. J. *27*, 379–423.

Shaw, S. L., Kamyar, R., and Ehrhardt, D. W. (2003). Sustained microtubule treadmilling in *Arabidopsis* cortical arrays. Science *300*, 1715–1718.

Sugimoto, K., Himmelspach, R., Williamson, R. E., and Wasteneys, G. O. (2003). Mutation or drug-dependent microtubule disruption causes radial swelling without altering parallel cellulose microfibril deposition in *Arabidopsis* root cells. Plant Cell *15*, 1414–1429.

Sunohara, H., Kawai, T., Shimizu-Sato, S., Sato, Y., Sato, K., and Kitano, H. (2009). A dominant mutation of TWISTED DWARF 1 encoding an alpha-tubulin protein causes severe dwarfism and right helical growth in rice. Genes Genet. Syst. *84*, 209–218.

Szymanski, D. B., and Cosgrove, D. J. (2009). Dynamic coordination of cytoskeletal and cell wall systems during plant cell morphogenesis. Curr. Biol. *19*, R800–R811.

Thitamadee, S., Tuchihara, K., and Hashimoto, T. (2002). Microtubule basis for left-handed helical growth in *Arabidopsis*. Nature *417*, 193–196.

Traas, J. A., Braat, P., and Derksen, J. W. (1984). Changes in microtubule arrays during the differentiation of cortical root cells of *Raphanus sativus*. Eur J. Cell Biol. *34*, 229–238.

Wasteneys, G. O. (2002). Microtubule organization in the green kingdom: chaos or self-order? J. Cell Sci. *115*, 1345–1354.

Wasteneys, G. O., and Ambrose, J. C. (2009). Spatial organization of plant cortical microtubules: close encounters of the 2D kind. Trends Cell Biol. *19*, 62–71.

Wasteneys, G. O., and Williamson, R. E. (1989a). Reassembly of microtubules in *Nitella tasmanica*—assembly of cortical microtubules in branching clusters and its relevance to steady-state microtubule assembly. J. Cell Sci. *93*, 705–714.

Wasteneys, G. O., and Williamson, R. E. (1989b). Reassembly of microtubules in *Nitella tasmanica*—quantitative-analysis of assembly and orientation. Eur. J. Cell Biol. *50*, 76–83.

Whittington, A. T., Vugrek, O., Wei, K. J., Hasenbein, N. G., Sugimoto, K., Rashbrooke, M. C., and Wasteneys, G. O. (2001). MOR1 is essential for organizing cortical microtubules in plants. Nature *411*, 610–613.

Wightman, R., and Turner, S. R. (2007). Severing at sites of microtubule crossover contributes to microtubule alignment in cortical arrays. Plant J. *52*, 742–751.

Yao, M., Wakamatsu, Y., Itoh, T. J., Shoji, T., and Hashimoto, T. (2008). *Arabidopsis* SPIRAL2 promotes uninterrupted microtubule growth by suppressing the pause state of microtubule dynamics. J. Cell Sci. *121*, 2372–2381.

Yuan, M., Shaw, P. J., Warn, R. M., and Lloyd, C. W. (1994). Dynamic reorientation of cortical microtubules, from transverse to longitudinal, in living plant cells. Proc. Natl. Acad. Sci. USA *91*, 6050–6053.